IJPSR (2013), Vol. 4, Issue 12 **(Research Article)**

INTERNATIONAL JOURNAL OF PHARMACEUTICAL SCIENCES AND RESEARCH

Received on 26 July, 2013; received in revised form, 29 September, 2013; accepted, 28 November, 2013; published 01 December, 2013

FORMULATION AND EVALUATION OF ENGINEERED PHARMACEUTICAL FINE PARTICLES OF BUDESONIDE FOR DRY POWDER INHALATION (DPI) PRODUCED BY AMPHIPHILIC CRYSTALLIZATION TECHNIQUE: OPTIMIZATION OF PROCESS PARAMETERS

P.S. Uttekar* and P.D. Chaudhari

Institute of Pharmacy, National Institute of Medical Sciences (NIMS) University, Shobhanagar, Jaipur, Rajasthan India

Keywords:
Budesonide, Dry Powder Inhalation, Amphiphilic Crystallization, Central Composite Design

Correspondence to Author:

Pravin S. Uttekar

Research Scholar, Institute of Pharmacy, NIMS University, Shobha Nagar, Jaipur-Delhi Highway (NH-11C), Jaipur – 303121, Rajasthan, India

E-mail: pravinsuttekar@yahoo.co.in

ABSTRACT: The purpose of this study was to produce of microparticles for Dry Powder Inhalation, produced by environmentally driven Amphiphilic crystallization technique process by using different nonionic surfactants at different concentration and at different processing parameters, for inhalation therapy. Budesonide, as one of the inhaled glucocorticosteroids, is widely used in the treatment of asthma by pulmonary delivery.The objective of the current work was to developed microcrystals by using Amphiphilic crystallization process with different nonionic surfactants at different processing parameters. Salvation of Budesonide in aqueous Cremophor EL and Tween 20(1:1) was investigated using HPLC. A response surface type central composite design were employed using Design-Expert 5.0 software (StatEase, QD Consulting, Penzance, UK) with the factors investigated were stirrer speed, antisolvent addition rate, Cremophor EL and Tween 20. The crystals were filtered and freeze dried. Optimize the process variables for narrow particle size distribution (PSD). Cremophor EL and Tween 20 were added as the stabilizers. Freeze dried crystals were subjected to XRD, DSC and SEM analysis for stability. The PSD also depended on the balance of meso and micromixing determined by the crystallization conditions. Optimized formulation was identified and characterized to determine their suitability for pulmonary delivery by using MSLI. Optimized formulation showed the highest FPF loaded and FPF emitted of 42 (1%) and 69 (3%) respectively, depositing mainly on stages 3 and 4, with much lower amounts collected on the higher stages of the MSLI.

INTRODUCTION: The topical delivery of corticosteroids by aerosols directly to the airways improves the pharmacological effect of the corticosteroids; aerosol delivery thereby prevents the systemic exposure and side effects. The alveolar epithelium is a potential absorption potential with respect to drug substances and macromolecules [1-2].

Budesonide is a potent glucocorticosteroid with high topical anti-inflammatory and low systemic effects; it has been widely used for treatment of asthma by inhalation administration with a variety of inhalation devices, including nebulizers, pressurized metered dose inhalers, and dry powder inhalers. Dry powder inhalation (DPI) has a better performance to deliver the drug because it is free

QUICK RESPONSE CODE

DOI: 10.13040/IJPSR.0975-8232.4(12).4656-70

Article can be accessed online on: www.ijpsr.com

DOI link: http://dx.doi.org/10.13040/IJPSR.0975-8232.4(12).4656-70

from the problems associated with the propellants used in comparison with the Metered Dose Inhaler (MDI) [3]. For effective deposition in the lower airways and deep lung, where drugs are most efficiently absorbed, the particle aerodynamic diameter (*D*ae) needs to be in the 1-5 μm range [4-17].

Drug particles in the range of 1–10 μm were produced by traditional micronization technique. Step of micronization is a size-reduction process which requires high energy; air-jet mill is a good example of traditionally micronization technique, which exhibits poor control over particle size and give wide distribution of particle size and shape. So the traditional micronization techniques influence the aerodynamic properties of particles [18-19].

Micronization of Active Pharmaceutical Ingredient provides amorphous nature, these solid-state transition convert Active Pharmaceutical Ingredient into the metastable phase form which is unstable form [20–23]. Milling processes is also resulted in the Polymorphic transitions of Active Pharmaceutical Ingredient and an alteration in particle surface energy has been measured following milling [24–29].

Crystal growth and agglomeration inhibition was the alternate strategies to control the Particle Size Distribution by the use of crystal growth inhibiting polymers; other ways are, the use of controlled mixing technologies; the application of ultrasound to accelerate diffusion and nucleation; and the use of supercritical fluid antisolvent technologies [30-34].

Rasenack [35] prepared micronized particles for pulmonary delivery using a controlled crystallization process. But 20 % of the budesonide particles were larger than 10 μm. Antisolvent precipitation is a simple and cost-effective method for preparing drug ultrafine particles with narrow particle size distributions.

Wang and co-workers successfully prepared 0.2-1.2 μm beclomethasone dipropionate particles, which can also be used as an inhaled glucocorticosteroid, by antisolvent precipitation [36].

The combination of amphiphilic polymers demonstrates notable powers of aqueous solubilisation for hydrophobic drug molecules. In present study, we use the combination of two different amphiphilic polymers for Cremophor EL and Tween 20.

In this paper the antisolvent precipitation approach to preparing budesonide powders suitable for dry powder inhalation is reported along with the solid-state properties and aerosol performance of the powders. In order to understand the manufacturing parameters controlling the crystal size distribution, factorial design of experiments was employed.

MATERIALS AND METHODS:

Materials: Budesonide was supplied from Sun Pharmaceutical Advanced Research Centre, Vadodara, Gujarat, Maharashtra, India. Cremophor EL were purchased from BASF *India* Limited Andheri (East), Mumbai, Maharashtra, India and Tween 20 were purchased from Sigma-Aldrich Chemie GmbH, Switzerland. Methanol (A.R. grade) was purchased from Loba Chemie Pvt. Ltd, Mumbai, India. Acetonitrile (CHROMASOLV, HPLC grade) was purchased from Sigma-Aldrich Co.

Powder Preparation:

Determination of the equilibrium solubility of Budesonide: Cremophor EL and Tween 20 (1:1) solutions in water were prepared by weighing appropriate amounts of Cremophor EL and Tween 20 (1:1) solution into volumetric flasks. Water was added to the solution of Cremophor EL and Tween 20 (1:1) to produce a series of weight/weight solutions (range 0–100% w/w solution of Cremophor EL and Tween 20 (1:1)). The solutions were mixed by using a magnetic stirrer (2MLH, Remi, India) plate. Each solution was transferred into a glass beaker and excess Budesonide was added. These suspensions were ultrasonicated for 2 min by using a Silverson L4RT Mixer with a high shear square hole head (Silverson Machines Ltd., Chesham, UK).

Aliquots of the suspensions were transferred to glass vials, to which excess drug was added and the vials were sealed. The suspensions were ultrasonicated ((BMI 599, Biomedica)) for 10 min to aid dispersion and dissolution. The suspensions were then placed in Orbital Shaker (Ris-24 BL, Remi, India) and were left to equilibrate for 72 h at

25°C. Samples were filtered through 0.45 µm cellulose acetate syringe filters into volumetric flasks.

Alternatively, for higher concentrations of Cremophor EL and Tween 20, samples were centrifuged at 1000 rmp for 5 min and the supernatant was transferred into volumetric flasks. Samples were diluted appropriately with mobile phase, and analyzed for drug content by high performance liquid chromatography (HPLC) according to a validated HPLC assay for Budesonide. All other chromatographic conditions were as reported previously and calibration curves were prepared for each fresh batch of mobile phase using calibration standards in the range 1–100 µg /ml Budesonide in mobile phase.

Crystallization of Budesonide:

a. **Preparation of Budesonide in Cremophor EL and Tween 20 (1:1) solutions:** Solutions of Budesonide were prepared by weighing the appropriate amount into a glass beaker and adding sufficient amount of solution of Cremophor EL and Tween 20 (1:1) to achieve the required concentration (% w/w). The beakers were covered with sealing film, and the solution was subjected to ultrasonication (BMI 599, Biomedica) for 5 min to aid Budesonide dispersion and dissolution. The solutions were then filtered using a 0.45 µm cellulose acetate syringe filter into glass vials and sealed.

b. **Amphiphilic crystallization of Budesonide:** The Cremophor EL and Tween 20 (1:1) solution was weighed into a standard 250 mL glass beaker. The beaker was placed on a laboratory elevator platform, under a Eurostar digitally controlled overhead stirrer (IKAwerk GmbH andCo. KG, Staufen, Germany) equipped with a stainless steel four blade turbine-propeller stirrer. The platform together with the beaker was raised, such that the propeller was positioned precisely at the centre. The vertical position of the stirrer was such that the underside of the stirrer was directly above the base of the beaker, but not in contact with the glass. Water was added as the antisolvent at a controlled rate using a model 505S peristaltic pump (Watson Marlow Bredel Pumps Ltd., Falmouth, UK). The antisolvent was directed to flow down the side wall of the glass beaker allowing initial contact with the surface of the Cremophor EL and Tween 20 solution at the beaker wall. The pump was calibrated for each desired flow rate, to ensure the addition of the correct weight of reverse osmosis water (filtered through a0.45 lm nylon membrane).

c. **Vacuum Filtration and drying:** After crystallization the crystals were separated by vacuum filtration using a0.45 lm nylon membrane filter (47 mm diameter) housed in a glass filter unit (Millipore (UK) Ltd., Watford, UK). The wet cake was washed with sufficient amount of water.The filter cake was put into the vacuum dryer (DZF-6050, Xinmiao, China) at 60 °C and -0.09 MPa for 12 h, and then the budesonide dry powder was obtained which was stored at room temperature over dried silica gel in a glass desiccator.

d. **Freeze Drying:** To investigate the process of particle formation, freeze drying was employed to obtain the powder any time during the Amphiphilic crystallization process. The suspensions containing budesonide particles were quickly frozen by liquid nitrogen (77K) and subsequently freeze dried with a freeze drier (LT-105, Christ, Germany) for 36-48 h, and then dry powder was obtained.

e. **Experimental design for the optimization of crystallization conditions:** A response surface type central composite design were employed using Design-Expert 5.0 software (StatEase, QD Consulting, Penzance, UK) with quadratic as design model. The factors investigated were stirrer speed and antisolvent addition rate, with both Cremophor EL and Tween 20 and the solution to antisolvent ratio held constant (5% w/w of Cremophor EL and Tween 20 (1:1)). The stirrer speeds investigated were 500(-1), 1000(0) and 1500 (1) rpm. The addition rate of waterwas studied at 10, 100.5 and 200 g min^{-1}.

Solid-State Characterization:

a. **X-ray Diffraction studies:** Powder X-ray patterns were recorded for pure drug and freeze dried product using a Bruker AXS diffractometer (Bruker AXS GmbH, Germany)

with a PSD-50M detector and EVA Application Software version6. Measurements were performed with a Cu Ka radiation source at 40 kV voltage, 30 mA current and a maximum scanning speed of 2^0/min.

b. **Differential Scanning Calorimetry:** DSC curves were obtained for pure drug and freeze dried product by a Differential Scanning Calorimeter (DSC 821e, Mettler-Toledo, Switzerland) at a heating rate of 5 K/min from 0 to 340^0C under nitrogen.

c. **Scanning Electron Microscopy:** Particle morphology was examined by scanning electron microscopy (SEM) (S250MK, Cambridge, U.K.) operating at 19 keV or SEM (JSM-6360LV, JEOL, Japan) operating at 20 keV. The pure drug and freeze dried powder could be characterized as dry powder. Samples were mounted on the copper stub by copper tape and sputter coated with Au at 6 mA for 3 min using a sputter coater (KYKY SBC-12, Beijing, China) under an Ar atmosphere.

d. **Bulk Density Determination:** The powders were subjected to bulk density and tapped density determination using Tapped density tester USP II (Veego, India).

e. **Particle size and distribution determination:** Particle sizing was carried out by laser diffraction using the Malvern MastersizerX (Malvern Instruments Ltd., Malvern, UK) equipped with a 100 mm focal length lens and anMS7 magnetically stirred cell using the 2 NHE software presentation. The sizing methods were validated according to ISO 13320 (1990) standards.

The crystals of budesonide (approximately 1 mg) were added to an 8 mL glass vial and 2 mL of filtered dispersant was added. The suspension was sonicated (BMI 599, Biomedica) in a water bath for 5 min to allow dispersion of the particles and aliquots were added successively to the sample cell by means of a Gilson pipette to achieve a satisfactory obscuration level (20% obscuration) and allowed to equilibrate for 60 s. Mean Particle size and Particle size distribution measurements were taken with each batch.

f. **Aerosol Performance:** The dispersion behaviour of the powder was assessed using an Aerolizer (Novartis Pharmaceutical, Australia) as the inhaler coupled through a USP stainless steel throat to a multistage liquid impinger (MSLI, Copley, U.K.), operating at 60 L/min controlled by the flow meter (DMF2000, Copley, U.K.) for 4 s. The MSLI is a versatile five-stage cascade impactor which can be used for determining the *D*ae distribution of Dry Powder Inhalation (DPI).

The design is such that at a flow rate of 60L/min, the cut off diameters of stages 1, 2, 3, and 4 are 13, 6.8, 3.1, and 1.7 μm, respectively. Stage 5 comprises an integral paper filter to capture the remaining fraction of particles less than 1.7 μm. By evaluating the DPI, it is then possible to calculate the mass fraction of drug particles smaller than 5 μ min the aerosol cloud, i.e., fine particle fraction (FPF). For MSLI, the FPF loaded and FPF emitted are defined as follows;

FPF Loaded=

$$\frac{\text{Powder mass on Stage 3 + Stage 4 + Filter}}{\text{Total Mass Recovered}} \quad \ldots\ldots 1$$

FPF=

$$\frac{\text{Powder mass on Stage 3 + Stage 4 + Filter}}{\text{Total Mass Recovered – Capsule and Device Retention}} \quad \ldots\ldots 2$$

Where, the capsule and device retention is the mass of drug remaining in the capsules and the device. Stages 1-4 of MSLI were injected into 20.0 mL of methanol via a 0-5000 μL pipet (Transforpette, Brand, Germany), and the filter stage of MSLI is covered with a GF/A filter paper (70mm, Whatman, U.K.). The powder (10.00 (0.50 mg) was filled into Vcaps capsules (size 3, Capsuge, Suzhou, China).

After analysis, the capsule, inhaler, throat, and filter paper were carefully rinsed with 20 mL of methanol. The MSLI itself was tightly sealed with Parafilm (Pechiney Plastic Packaging, USA) to avoid evaporation losses and gently shaken for 5-10 min to dissolve drug from each stage. Each experiment was performed in duplicate. Budesonide deposited at different locations was assayed by HPLC (Alliance 2695, Waters, USA)

using a reverse-phase column (SunFire, Waters, USA) and a PDA UV detector (2996, Waters, USA) at 245.5 nm. The mobile phase was (acetonitrile: water) 40:60 (%) and the flow rate was 1 mL/min. A linear calibration plot of budesonide in methanol was constructed in the concentration range of 11-168 μg/ml [Area) 1.792053e6 × concentration (mg/mL)-1.531721e3, *R*2) 0.999996, *n) 3*].

RESULTS AND DISCUSSION:

Solubilization of Budesonide by Cremophor EL and Tween 20: We investigated the solubility of budesonide in solution of Cremophor EL and Tween 20 (1:1) as a crystallizing solvent for the amphiphilic crystallization technique. A logarithmic increase in the solubility of budesonide with increasing concentration of Cremophor EL and Tween 20 (1:1) solution in water as achieved (**Figure 1**). The plot of logarithm of the solubility (S) of budesonide displayed a linear relationship with Cremophor EL and Tween 20 (1:1) solution concentration (r2 = 0.854). The regression equation for the solubility in the co-solvent system was -

$$y = 0.023x + 1.615 \quad \ldots\ldots\ldots\ldots\ldots\ldots\ldots\ldots (3)$$

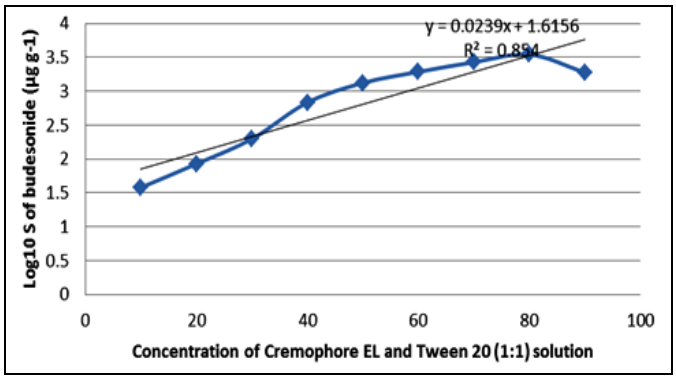

FIGURE 1: THE LOG10 SOLUBILITY (S) OF BUDESONIDE AS A FUNCTION OF CONCENTRATION OF CREMOPHOR EL AND TWEEN 20 (1:1) SOLUTION (EACH DATA POINT REPRESENTS THE MEAN ± SD, nP3).

However, the regression analysis revealed a significant lack of fit ($p < 0.001$). Cremophor EL and Tween 20 solubilized Budesonide with a typical log-linear increase in solubility as Cremophor EL and Tween 20 (1:1) concentration increased [37]. There is an approximately 1000-fold difference between the solubility of Budesonide in solution of Cremophor EL and Tween 20 (1:1) and in pure water [38].

The decline curve after 80% concentration of Solutions of Cremophor EL and Tween 20 (1:1) in water was an evidence of specific solvation interactions existence (e.g. H-bonding). Solutions of Cremophor EL and Tween 20 (1:1) in water show extensive interactions in the form of intermolecular H-bonds which break down the structure of water and hence facilitate an increase in solubility of Budesonide [39-42].

Solid-State Characterization:

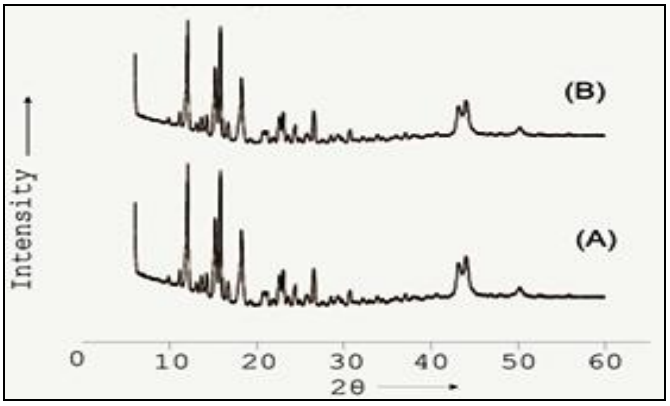

FIGURE 2: X-RAY DIFFRACTION PATTERNS OF VARIOUS BUDESONIDE DRY POWDERS: (A) COMMERCIAL BUDESONIDE PRODUCT; (B) FREEZE DRIED PRODUCT

As shown in **Figure 2A and 2B**, represents budesonide pure drug and freeze dried powder respectively. Budesonide pure drug and freeze dried powder were of represents same X-ray diffraction patterns, which indicated that there were no changes in crystal structure after the antisolvent precipitation process in the presence of stabilizers i.e. Cremophor EL and Tween 20. Although the intensities of some diffraction peaks of as freeze dried product were relatively weak compared with the commercial budesonide pure, it could be explained by the great decrease of particle size.

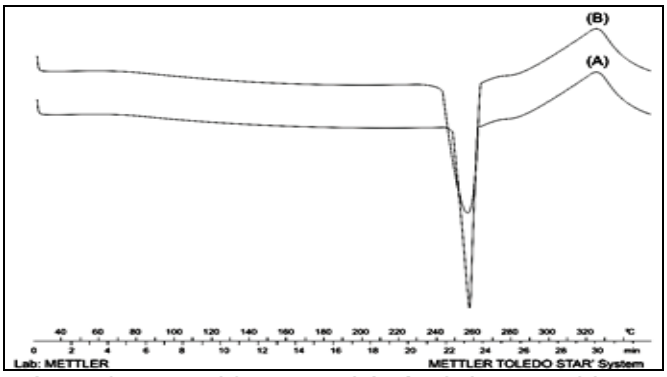

FIGURE 3: THE DSC THERMOGRAMS OF BUDESONIDE PURE (A) AND FREEZE DRIED POWDER (B)

Thermogram of budesonide pure has shown sharp melting endotherm at 257.4^{o}C. A diffused peak with less intense peak at 256.9^{o}C in thermogram of freeze dried powder confirms the presence of drug with impurities and slight transition towards amorphous nature. Slight amorphous structure attributes that the **budesonide** being dissolved in the solid-state carrier matrix present trace amount in powder (Figure 3). When the budesonide solution was mixed with water, the liquid was turbid immediately, which indicated the onset of precipitation. Less onset of precipitation has higher possibilities to generate a non-crystalline solid during such a rapid precipitation process because budesonide molecules would lose mobility before assuming their lattice positions. Then on crystalline material is considered amorphous because it lacks long-range order.

As shown in Figure 2A, initially particles were of crystalline in nature the freeze-dried powder from such suspensions was confirmed to be completely amorphous because only one broad and dispersed maximum peak was detected in the pattern (Figure 4B). Amorphous materials have higher Gibbs free energies than crystals. Thermodynamic laws predict that materials seek to minimize their free energies by transitioning to lower energy states (e.g., crystallization), which leads to physical instability of the drug. Therefore, crystalline budesonide is preferable. The budesonide particles were be fully crystallized after continuous stirring for 5 min with freeze drying thereafter [43].

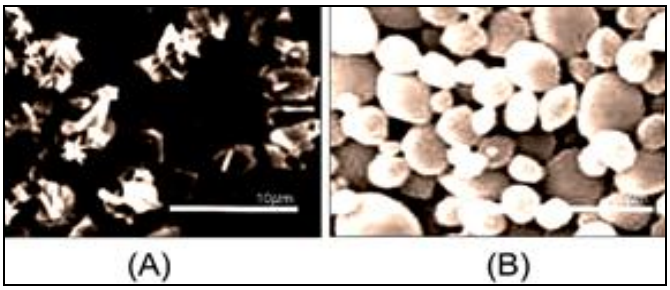

FIGURE 4: SEM PHOTOGRAPHS OF VARIOUS BUDESONIDE PARTICLES: (A) PURE DRUG; (B) FREEZE DRIED POWDER.

A comparison of **Figure 4a and 4b** reveals the effect of the stabilizer on the crystal habit. Crystals of rectangular shape (less than 5 μm in length and 300 nm in thickness) were of pure drug and oval shape particles were obtained from amphiphilic crystallization technique by using stabilizers i.e Cremophor EL and Tween 20.

The SEM images indicates that the presence of lots of agglomerates formed by crystal bridges between the flaky particles of the pure drug. Whereas the powder produce by amphiphilic crystallization technique is free from agglomerates this can be explained by the occurrence of recrystallization at the proper contact point between particles [44].

Budesonide particles from pure drug and powder produced by amphiphilic crystallization technique had similar major diameters but narrower distribution. The agglomerates formed by the flaky particles of pure drug had a rough surface, which effectively decreases the interagglomerate distance and increase the van der Waals attractive force. Furthermore, the surface asperities may also increase the effective area of contact between agglomerates. Namely, the agglomerates of pure drug had a higher bulk density and tapped density i.e 0.76 g/cc $\pm$ 0.2 and 0.72 g/cc $\pm$ 0.5 respectively. Although the Ultrafine oval shape budesonide particles produced by amphiphilic crystallization technique have less bulk and tapped density i.e 0.46 g/cc $\pm$ 0.3 and 0.52 g/cc $\pm$ 0.4 respectively with good flowing characteristics [45-46].

Response surface construction to optimize crystallization parameters: The mean and standard deviation of particle size of budesonide obtained by using controlled crystallization technique with use of combination of Cremophor EL and Tween 20 (%) was studied. There is also brief elaboration of effect of Antisolvent Addition Rate (ml/min) & Stirring Speed (rpm) on crystal growth. For the optimization purpose we select Central Composite Design (**Table 1 & 2**) with Quadratic and 2FI as design model from mean particle size and standard deviation of mean particle size respectively for response surface category (Table 2).

It gives 30 runs, with no blocks in the design. Four factors i.e. Cremophor EL (%), Tween 20 (%), Antisolvant Adition Rate (ml/min) & Stirring Speed (rpm) to be considered as independable variables. Response for mean particle size (Dependable Variable 1) and standard deviation (Dependable Variable 2) of mean particle size was analyzed with polynomial. Dependable Variable 1 ranges from 1.30 to 9.200 and for dependable Variable 2 it was from 0.30 to 10.40. Current design models do not required data transformation.

TABLE 1: EXPERIMENTAL RUNS ACCORDING TO CENTRAL COMPOSITE DESIGN WITH THEIR CODED VALUES

Standard	Runs	A: Cremophor EL (%)	B: Tween 20 (%)	C: Antisolvent Addition Rate (ml/min)	D: Stirring Speed (rpm)	Mean Particle Size	Standard Deviation
23	7	0.00	0.00	0.00	-2.00	5.3	3.9
1	15	-1.00	-1.00	-1.00	-1.00	9.2	8.5
2	24	1.00	-1.00	-1.00	-1.00	4.7	7.5
3	5	-1.00	1.00	-1.00	-1.00	6	1.5
4	27	1.00	1.00	-1.00	-1.00	2.1	0.3
5	1	-1.00	-1.00	1.00	-1.00	6.2	9.6
6	8	1.00	-1.00	1.00	-1.00	5.3	5.4
7	28	-1.00	1.00	1.00	-1.00	3.1	3.6
8	30	1.00	1.00	1.00	-1.00	3.6	2.4
17	21	-2.00	0.00	0.00	0.00	7.8	3.5
18	11	2.00	0.00	0.00	0.00	1.3	2.6
19	23	0.00	-2.00	0.00	0.00	4.1	5.7
20	13	0.00	2.00	0.00	0.00	2.6	1.2
21	17	0.00	0.00	-2.00	0.00	2.9	3.5
22	3	0.00	0.00	2.00	0.00	2.1	4.2
25	14	0.00	0.00	0.00	0.00	3.4	4.7
26	18	0.00	0.00	0.00	0.00	3.4	4.7
27	22	0.00	0.00	0.00	0.00	3.4	4.7
28	16	0.00	0.00	0.00	0.00	3.4	4.7
29	9	0.00	0.00	0.00	0.00	3.4	4.7
30	25	0.00	0.00	0.00	0.00	3.4	4.7
9	6	-1.00	-1.00	-1.00	1.00	8.4	10.4
10	19	1.00	-1.00	-1.00	1.00	4.9	5.3
11	10	-1.00	1.00	-1.00	1.00	2.5	5.7
12	20	1.00	1.00	-1.00	1.00	2.3	3.6
13	29	-1.00	-1.00	1.00	1.00	7.3	7.5
14	26	1.00	-1.00	1.00	1.00	4.7	4.3
15	2	-1.00	1.00	1.00	1.00	5.8	2.6
16	4	1.00	1.00	1.00	1.00	3.7	5.3
24	12	0.00	0.00	0.00	2.00	6.8	4.2

TABLE 2: DESIGN SUMMARY FOR 30 RUNS WITH QUADRATIC AND 2FI AS DESIGN MODELS.

Factor	Name	Units	Type	Low Actual	High Actual	Low Coded	High Coded	Mean	Std. Dev.
A	Cremophor EL	%	Numeric	-1.00	1.00	-1.000	1.000	0.000	0.894
B	Tween 20	%	Numeric	-1.00	1.00	-1.000	1.000	0.000	0.894
C	Addition rate	ml/min	Numeric	-1.00	1.00	-1.000	1.000	0.000	0.894
D	Stirrer Speed	rpm	Numeric	-1.00	1.00	-1.000	1.000	0.000	0.894

Response	Name	Analysis	Min.	Max.	Mean	Std. Dev.	Ratio	Trans	Model
Y1	Mean Particle Size	Polynomial	1.30	9.200	4.437	1.97	7.077	None	Quadratic
Y2	Standard Deviation of mean particle size	Polynomial	0.30	10.40	4.683	2.25	34.66	None	2FI

Optimization of process parameters for Mean Particle size

(Dependable variable 1) - Correlation of Cremophor EL was -0.570, Tween 20 was -0.464, addition rate was -0.038, and stirrer speed was 0.045 with Mean Particle size (Dependable variable 1) shown in **Figure 5, Figure 6, Figure 7 and Figure 8** respectively. Cremophor EL, Tween 20 and addition rate shows negative correlation with respect to mean particle size; reversely stirrer speed shows positive correlation.

As the high amount of Cremophor EL, Tween 20 and high addition rate decreases the particle size and high stirrer speed gives coarse particles.

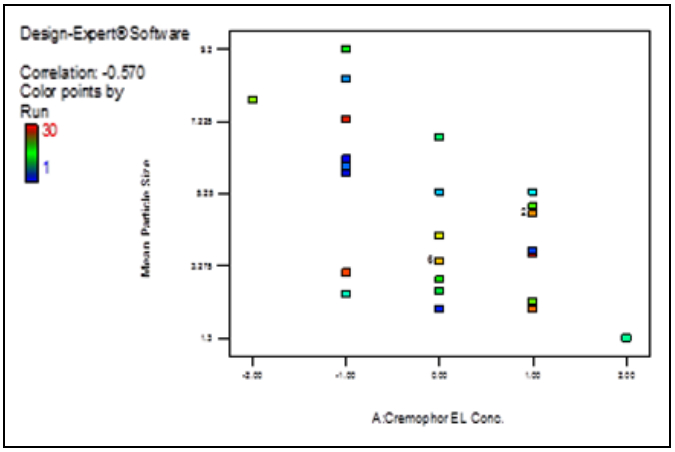

FIGURE 5: GRAPHS SHOWING CORRELATION BETWEEN CREMOPHOR EL AND MEAN PARTICLE SIZE

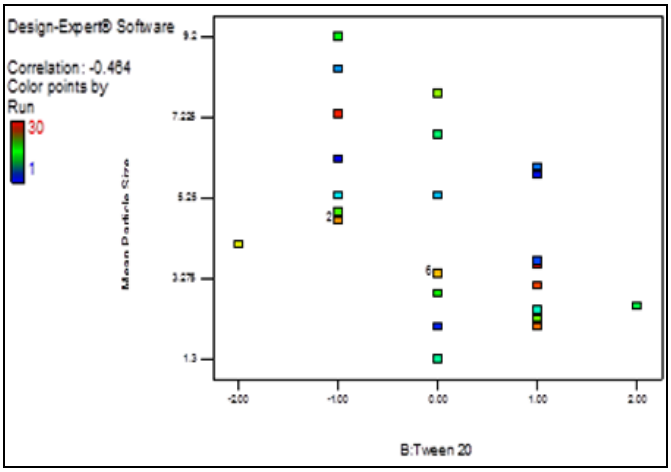

FIGURE 6: GRAPHS SHOWING CORRELATION BETWEEN TWEEN 20 AND MEAN PARTICLE SIZE

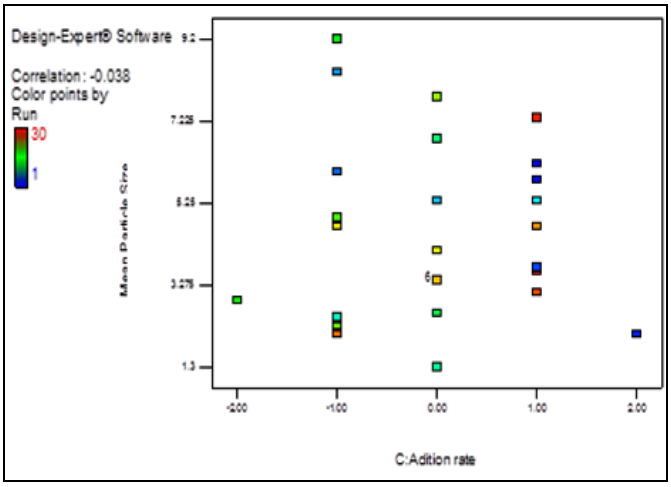

FIGURE 7: GRAPHS SHOWING CORRELATION BETWEEN ADDITION RATE AND MEAN PARTICLE SIZE

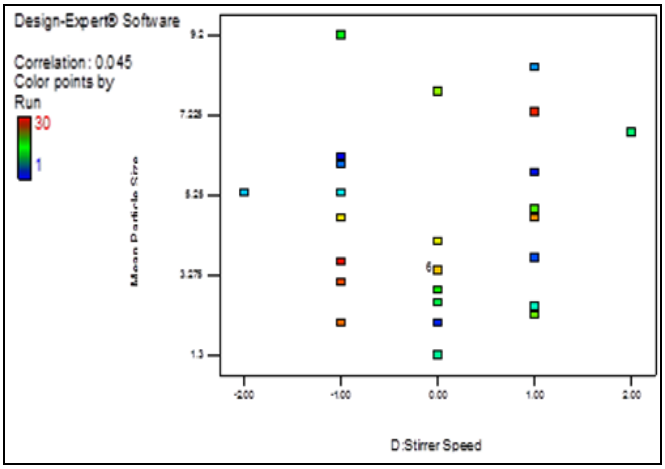

FIGURE 8: GRAPHS SHOWING CORRELATION BETWEEN STIRRER SPEED AND MEAN PARTICLE SIZE

The cubic model is aliased. This means not enough experiments have been run to independently estimate all the terms for this model. The suggested model is Quadratic (**Table 3 and 4**).

TABLE 3: SEQUENTIAL MODEL SUM OF SQUARES [TYPE I] FOR MEAN PARTICLE SIZE

Source	Sum of Squares	df	Mean Square	F Value	p-value Prob > F	
Mean vs Total	590.52	1	590.52			
Linear vs Mean	63.62	4	15.91	7.43	0.0004	Suggested
2FI vs Linear	11.49	6	1.91	0.87	0.5377	
Quadratic vs 2FI	22.31	4	5.58	4.24	0.0171	Suggested
Cubic vs Quadratic	14.83	8	1.85	2.65	0.1081	Aliased
Residual	4.89	7	0.70			
Total	707.67	30	23.59			

TABLE 4: MODEL SUMMARY STATISTICS FOR MEAN PARTICLE SIZE

Source	Std. Dev.	R-Squared	Adjusted R-Squared	Predicted R-Squared	PRESS	
Linear	1.46	0.5431	0.4700	0.3132	80.46	Suggested
2FI	1.49	0.6412	0.4523	-0.0535	123.42	
Quadratic	1.15	0.8316	0.6745	0.0302	113.62	Suggested
Cubic	0.84	0.9582	0.8270	-5.0149	704.64	Aliased

ANOVA (**Table 5**) suggested for the design is as follows. The Model F-value of 5.29 implies the model is significant. There is only a 0.14% chance that a "Model F-Value" this large could occur due to noise. Values of "Prob > F" less than 0.0500 indicate model terms are significant. In this case A, B, D2 are significant model terms. Contour plot is also given in figure 9.

TABLE 5: ANOVA FOR RESPONSE SURFACE QUADRATIC MODEL ANALYSIS OF VARIANCE TABLE [PARTIAL SUM OF SQUARES - TYPE III] FOR MEAN PARTICLE SIZE

Source	Sum of Squares	df	Mean Square	F -Value	p-value Prob > F	
Model	97.42	14	6.96	5.29	0.0014	
A-Cremophor EL Conc.	38.00	1	38.00	28.90	< 0.0001	
B-Tween 20	25.22	1	25.22	19.17	0.0005	
C-Adition rate	0.17	1	0.17	0.13	0.7268	
D-Stirrer Speed	0.24	1	0.24	0.18	0.6753	
AB	2.10	1	2.10	1.60	0.2254	
AC	3.06	1	3.06	2.33	0.1478	
AD	0.010	1	0.010	7.605E-003	0.9317	
BC	3.06	1	3.06	2.33	0.1478	
BD	0.010	1	0.010	7.605E-003	0.9317	**Significant**
CD	3.24	1	3.24	2.46	0.1373	
A2	5.15	1	5.15	3.92	0.0665	
B2	0.49	1	0.49	0.37	0.5517	
C2	0.17	1	0.17	0.13	0.7227	
D2	17.92	1	17.92	13.63	0.0022	
Residual	19.72	15	1.31			
Lack of Fit	19.72	10	1.97			
Pure Error	0.000	5	0.000			
Cor Total	117.15	29				

Final Equation in Terms of Coded Factors:

Mean Particle Size =
+3.40
-1.26 * A
-1.03 * B
-0.083 * C
+0.10 * D
+0.36 * A * B
+0.44 * A * C
+0.025 * A * D
+0.44 * B * C
-0.025 * B * D
+0.45 * C * D
+0.43 * A2
+0.13 * B2
-0.079 * C2
+0.81 * D2……(4)

Final Equation in Terms of Actual Factors:

Mean Particle Size =
+3.40000
-1.25833 * Cremophor EL Conc.
-1.02500 * Tween 20
-0.083333 * Addition rate
+0.10000 * Stirrer Speed
+0.36250 * Cremophor EL Conc. * Tween 20
+0.43750 * Cremophor EL Conc. * Addition rate
+0.025000 * Cremophor EL Conc. * Stirrer Speed
+0.43750 * Tween 20 * Addition rate
-0.025000 * Tween 20 * Stirrer Speed
+0.45000 * Addition rate * Stirrer Speed
+0.43333 * Cremophor EL Conc.^{2}
+0.13333 * Tween 20^2
-0.079167 * Addition rate^2
+0.80833 * Stirrer Speed^2……..(5)

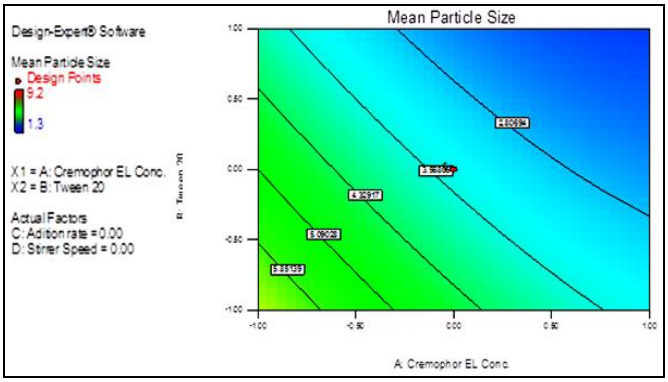

FIGURE 9: RESPONSE SURFACE GRAPH FOR MEAN PARTICLE SIZE WITH RESPECT TO CREMOPHOR EL AND TWEEN 20 CONC. AS A PROMINENT FACTORS

Optimization of process parameters for Standard Deviation of Mean Particle size (Response – 2) – Correlation of Cremophor EL was -0.283, Tween 20 was -0.703, addition rate was -0.012, and stirrer speed was 0.107 with standard deviation of Mean Particle size (Dependable variable 2) shown in **Figure 10, Figure 11, Figure 12 and Figure 13** respectively.

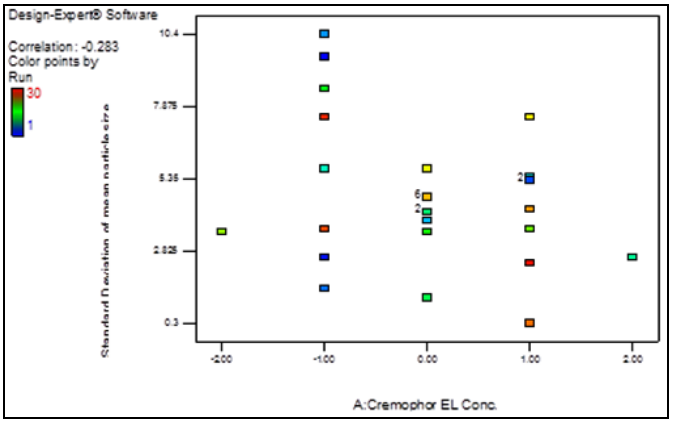

FIGURE 10: GRAPHS SHOWING CORRELATION BETWEEN CREMOPHOR EL AND STANDARD DEVIATION OF MEAN PARTICLE SIZE

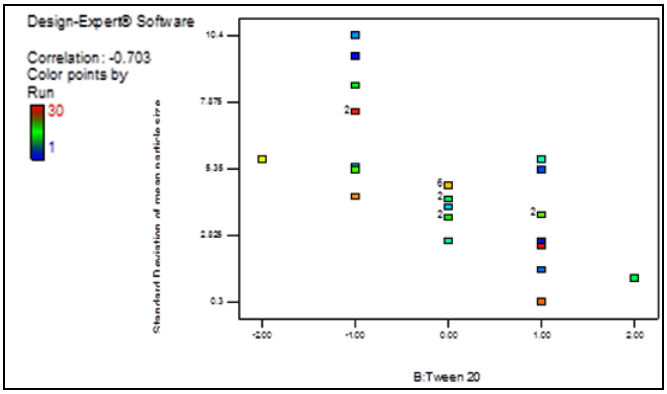

FIGURE 11: GRAPHS SHOWING CORRELATION BETWEEN TWEEN 20 AND STANDARD DEVIATION OF MEAN PARTICLE SIZE

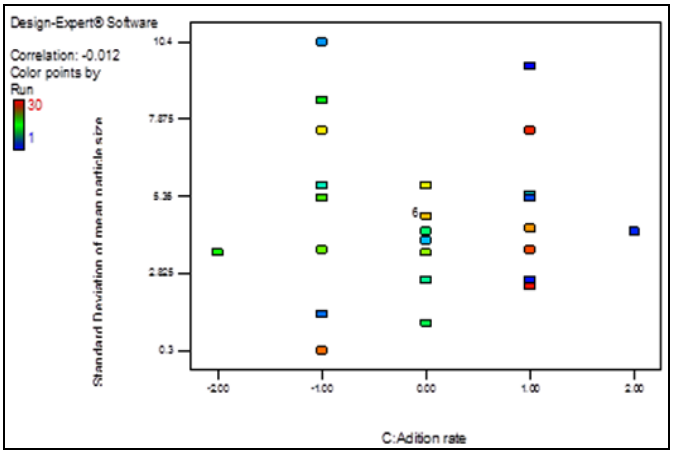

FIGURE 12: GRAPHS SHOWING CORRELATION BETWEEN ADDITION RATE AND STANDARD DEVIATION OF MEAN PARTICLE SIZE

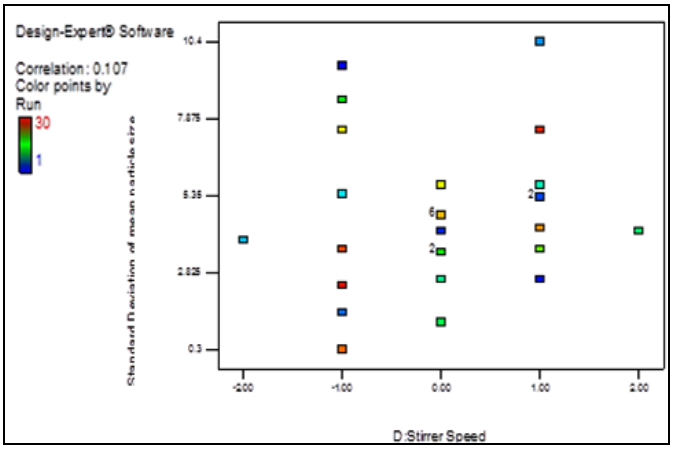

FIGURE 13: GRAPHS SHOWING CORRELATION BETWEEN STIRRER SPEED AND STANDARD DEVIATION OF MEAN PARTICLE SIZE

The cubic model is aliased. This means not enough experiments have been run independently estimate all the terms for this model. The suggested model is 2FI (**Table 6 and 7**).

TABLE 6: SEQUENTIAL MODEL SUM OF SQUARES [TYPE I] FOR STANDARD DEVIATION OF MEAN PARTICLE SIZE

Source	Sum of Squares	df	Mean Square	F Value	p-value Prob > F	
Mean vs Total	658.01	1	658.01			
Linear vs Mean	89.22	4	22.31	8.83	0.0001	Suggested
2FI vs Linear	27.94	6	4.66	2.51	0.0582	Suggested
Quadratic vs 2FI	1.18	4	0.30	0.13	0.9690	
Cubic vs Quadratic	20.05	8	2.51	1.25	0.3888	Aliased
Residual	13.98	7	2.00			
Total	810.39	30	27.01			

TABLE 7: MODEL SUMMARY STATISTICS FOR STANDARD DEVIATION OF MEAN PARTICLE SIZE

Source	Std. Dev.	R-Squared	Adjusted R-Squared	Predicted R-Squared	Press	
Linear	1.59	0.5855	0.5192	0.3524	98.68	Suggested
2FI	1.36	0.7689	0.6473	0.1496	129.58	Suggested
Quadratic	1.51	0.7767	0.5682	-0.2864	196.02	
Cubic	1.41	0.9083	0.6199	-12.2118	2013.24	Aliased

ANOVA (**Table 8**) suggested for the design is as follows. The Model F-value of 6.32 implies the model is significant. There is only a 0.03% chance that a "Model F-Value" this large could occur due to noise. Values of "Prob > F" less than 0.0500 indicate model terms are significant. In this case A, B, AB, BD are significant model terms. Contour plot is also given in **figure 14**.

TABLE 8: ANOVA FOR RESPONSE SURFACE 2FI MODEL ANALYSIS OF VARIANCE TABLE [PARTIAL SUM OF SQUARES - TYPE III] FOR STANDARD DEVIATION OF MEAN PARTICLE SIZE

Source	Sum of Squares	df	Mean Square	F Value	p-value Prob > F	
Model	117.17	10	11.72	6.32	0.0003	
A-Cremophor EL Conc.	12.18	1	12.18	6.57	0.0190	
B-Tween 20	75.26	1	75.26	40.61	< 0.0001	
C-Addition rate	0.020	1	0.020	0.011	0.9175	
D-Stirrer Speed	1.76	1	1.76	0.95	0.3420	
AB	8.56	1	8.56	4.62	0.0448	
AC	0.77	1	0.77	0.41	0.5281	
AD	6.250E-004	1	6.250E-004	3.372E-004	0.9855	Significant
BC	3.71	1	3.71	2.00	0.1735	
BD	10.40	1	10.40	5.61	0.0286	
CD	4.52	1	4.52	2.44	0.1350	
Residual	35.21	19	1.85			
Lack of Fit	35.21	14	2.52			
Pure Error	0.000	5	0.000			
Cor Total	152.38	29				

Final Equation in Terms of Coded Factors:

Standard Deviation of mean particle size =

+4.68
-0.71 * A
-1.77 * B
-0.029 * C
+0.27 * D
+0.73 * A * B
+0.22 * A * C
-6.250E-003 * A * D
+0.48 * B * C
+0.81 * B * D
-0.53 * C * D……(6)

Final Equation in Terms of Actual Factors:

Standard Deviation of mean particle size =

+4.68333
-0.71250 * Cremophor EL Conc.
-1.77083 * Tween 20
-0.029167 * Addition rate
+0.27083 * Stirrer Speed
+0.73125 * Cremophor EL Conc. * Tween20
+0.21875 * Cremophor EL Conc. * Addition rate
-6.25000E-003 * Cremophor EL Conc. * Stirrer Speed
+0.48125 * Tween 20 * Addition rate
+0.80625 * Tween 20 * Stirrer Speed
-0.53125 * Addition rate * Stirrer Speed……(7)

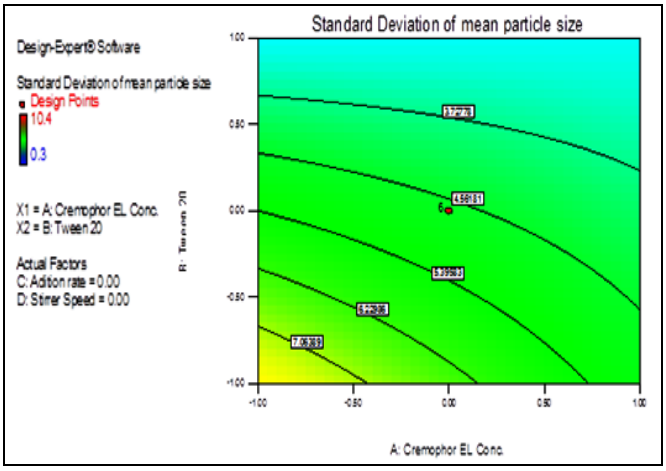

FIGURE 14: RESPONSE SURFACE GRAPH FOR STANDARD DEVIATION OF MEAN PARTICLE SIZE WITH RESPECT TO CREMOPHOR EL AND TWEEN 20 CONC. AS A PROMINENT FACTORS

Cremophor EL and Tween 20 were chosen as the stabilizing agents because of their good stabilizing properties and low toxicity. Owing to the different molecular structures, composition and molecular weight, the prepared budesonide particles were somewhat less than 5 μm. Cremophor EL and Tween 20 both reduce the particle size by hydrodynamic force. The large molecule of the stabilizer would be adsorbed on the surface of particles so that the recrystallization process at the

cross-contact point between particles would be prevented, and thus, individual particles were produced.

The main component of Cremophor EL is glycerol polyethylenenglycol ricinoleate. Together with fatty acid esters of polyethylene glycol, this forms the hydrophobic part of the product. The smaller hydrophilic part consists of free polyethylene glycols and ethoxylated glycerol. Because of smaller hydrophilic part of the Cremophor EL we used Tween 20 in combination to modify the hydrophilic properties of Cremophor EL and thereby solubility.

Tween 20 is a polyoxyethylene derivative of sorbitan monolaurate, and is distinguished from the other members in the polysorbate range by the length of the polyoxyethylene chain and the fatty acid ester moiety. Combination of Cremophor EL and Tween 20 was imparting highest solubility for the drug [47].

Cremophor EL has highest impact on the decreasing mean particle size and that of lesser on standard deviation as reversely that of Tween 20 (figure 9 and 14). Tween 20 decreasing standard deviation of mean particle size as shown in the equation 4, 5, 6 and 7.

Supersaturation state further leads to generation of small crystals and it further consumed by nucleation stage. After nucleation state further crystal growth is there. Crystal size and distribution depends on the rate of supersaturation and thereby nucleation. Thus the addition rate further improves the mean particle size and their standard deviation as shown in the equation 4, 5, 6 and 7. Higher addition rate of antisolvent decreases the mean particle size by increased rate of supersaturation and thereby nucleation. The smaller particles produced by high addition rate also stabilized by the stabilizers added i.e. Cremophor EL and Tween 20 [48].

The final Particle Size Distribution in a precipitation process is determined by the relative balance of the kinetic rates of nucleation and crystal growth. The Particle Size Distribution, however, is dependent on the initial number of nuclei formed and also on the growth rate of those nuclei [49].

However, Cremophor EL and Tween 20 demonstrates a higher viscosity than most conventional solvents, and the difference in viscosity between Cremophor EL and Tween 20 with respect to water renders rapid homogeneous liquid mixing difficult. The Cremophor EL and Tween 20 –water system demonstrated a balance between micromixing and mesomixing (a larger scale mass transfer of the antisolvent). The lower rate of micromixing in viscous systems ensures a competition between micromixing and nucleation leading to a low nucleation rate at low antisolvent addition rates [50].

Thus supersaturation can be consumed by crystal growth leading to higher particle sizes. As the antisolvent addition rate is increased, a shift in the balance of micro- to mesomixing occurs. Mesomixing leads to localization of high levels of supersaturation in turbulent eddies and concomitant high rates of nucleation. Thus large numbers of primary nuclei are formed which possess a large surface area, and undergo limited growth in regions of lower local supersaturation leading to a narrow particle size distribution [51].

Stirring improves micromixing but lowers local supersaturation by facilitating turbulent mesomixing and thereby crystal growth was a resultant effect and the mean particle size to be increased as shown in the equation 4, 5, 6 and 7. Crystal growth involves an element of volume-diffusion control where solute molecules must diffuse through a diffusion barrier around nascent crystals. Increasing the stirring speed facilitates diffusion by decreasing the thickness of the stagnant boundary layer, hence affecting the balance between nucleation and crystal growth. Both of these reasons stirring speed broaden particle size distribution [52].

Selection of optimized formulation - We set constrains for the Independent variables (**Table 9**). In order to achieve of targeted response i.e. minimum mean particle size and their standard deviation, the 41 solutions suggested by the Design Expert software with descending order of desirability. Form the 41 solutions first 10 solutions with high desirability were sown in **Table 10.** From solutions the solution with highest desirability we selected as optimized formulation i.e. F1 formulation.

TABLE 9: CONSTRAINTS FOR THE VARIABLES

Name	Goal	Lower Limit	Upper Limit	Lower Weight	Upper Weight	Importance
Cremophor EL Conc.	is in range	-1	1	1	1	3
Tween 20	is in range	-1	1	1	1	3
Adition rate	maximize	-1	1	1	1	3
Stirrer Speed	minimize	-1	1	1	1	3
Mean Particle Size	minimize	1	5	1	1	3
Standard Deviation of mean particle size	minimize	0.3	10.4	1	1	3

TABLE 10: FORMULATIONS (UP TO 10) ACCORDING TO THE DESCENDING ORDER OF DESIRABILITY

Number	Cremophor EL	Tween 20	Addition rate	Stirrer Speed	Mean Particle Size	Standard Deviation of mean particle size	Desirability
F1	0.49	1.00	1.00	-1.00	2.93391	2.9374	0.786
F2	0.50	1.00	1.00	-1.00	2.93323	2.94239	0.786
F3	0.52	1.00	1.00	-1.00	2.93262	2.94494	0.786
F4	0.48	1.00	1.00	-0.99	2.92921	2.93868	0.786
F5	0.46	1.00	1.00	-0.99	2.92802	2.93525	0.786
F6	0.40	1.00	1.00	-1.00	2.94328	2.91514	0.786
F7	0.59	1.00	1.00	-1.00	2.93233	2.96205	0.785
F8	0.33	1.00	1.00	-1.00	2.95241	2.90055	0.785
F9	0.51	0.98	1.00	-1.00	2.93463	2.97365	0.785
F10	0.64	1.00	1.00	-1.00	2.9348	2.97474	0.785

Inhalation Properties - Optimised formulation F1 had evaluated by the deposition pattern by MSLI. The results indicated that the budesonide particles of less fine fraction and spherical morphology had shown significantly better aerosol performance. Optimized product corresponding to a decrease in stage 1 deposition along with a subsequent increase in stages 3 and 4 in the MSLI. It is worth that the particles were uniform in the presence of Cremophor EL and Tween 20 showed the highest FPF loaded and FPF emitted of 42 (1%) and 69 (3%) respectively, depositing mainly on stages 3 and 4, with much lower amounts collected on the higher stages of the MSLI.

According to definition of D_{ae};

$$Dae = Deq\sqrt{\frac{\rho p}{\rho 0x}} \quad \text{.....(8)}$$

$$Deq = 3\sqrt{\frac{6V}{\pi}} \quad \text{.....(9)}$$

Where, *D*eq is the volume-equivalent diameter of the particle, *V* is the particle volume, ρ_p is the particle bulk density, ρ_0 is the unit density, and χ is the dynamic shape factor, defined as the ratio of the drag force on a particle to the drag force on the particle volume-equivalent sphere at the same velocity. Thus, *D*ae can be reduced by one or more of the following manipulations :(1) decreasing the volume-equivalent particle diameter(*D*eq), (2) reducing the particle density (ρ_p), and (3) increasing the particle dynamic shape factor (χ). Optimized budesonide particles had the thin thickness, and the spherical particles were calculated to be of higher *D*eq.

The agglomerates formed by the spherical particles had a smooth surface, which effectively increased the interagglomerate distance and lowered the van der Waals attractive force. Furthermore, the surface asperities may also reduce the effective area of contact between agglomerates. Namely, the agglomerates had a lower bulk density. Third, the χ value for the particles of spherical shapes could be smaller. On account of the above reasons, the *D*ae of these spherical particles was intermediate so that they had high FPF values.[53]

CONCLUSION: Combination of Cremophor EL and Tween 20 has been shown to be eminently suitable stabilizer in a amphiphilic crystallization technique for budesonide. Maximal solubility of budesonide in combination of Cremophor EL and Tween 20 solution due to different hydrophilic and hydrophobic character enabled the production of microparticles suitable for exploitation in topical lung drug delivery according to a novel and

environmentally benign production method of amphiphilic crystallization. Physical Stability of freeze dried product was confirmed by XRD, DS and SEM. The PSD was shown to depend on the hydrodynamic conditions provided by the Cremophor EL and Tween 20 which acts as stabilizers and did not require the use of traditional crystallization inhibitors. Stabilizers played important roles in the formation and growth of budesonide particles.

In this study the factors i.e. Cremophor EL (%), Tween 20 (%), Antisolvent Addition Rate (ml/min) & Stirring Speed (rpm) controlling the microcrystallization of budesonide by amphiphilic crystallization have been identified. Optimized formulation was identified and characterized to determine their suitability for pulmonary delivery by using MSLI. Higher FPF values were performed by the agglomerates formed by spherical particles had intermediate volume-equivalent particle diameter with less standard deviation, lower bulk density, and larger dynamic shape factor. The antisolvent precipitation due to its being simple and cost effective will be a prosperous pathway of budesonide preparation for DPI application.

ACKNOWLEDGMENT: Authors are very thankful of Sun Pharmaceutical Advanced Research Centre, Vadodara, Gujarat, Maharashtra, India for providing Budesonide a gift sample for the study.

REFERENCES:

1. Gumbleton M., Taylor G., Challenges and innovations in effective pulmonary systemic and macromolecular drug delivery, Advanced Drug Delivery Review 2006; 58: 993–995.
2. Forbes B., Ehrhardt C., Human respiratory epithelial cell culture for drug delivery applications, European Journal of Pharmaceutics and Biopharmceutics 2005; 60: 193–205.
3. Hickey A, Pharmaceutical inhalation aerosol technology, 2nd Ed. New York, NY: Marcel Dekker, Inc. 2004. 603.
4. Dunbar C., Holzner P., Dispersion and characterization of pharmaceutical dry powder aerosols, KONA Powder Part 1998; 16:7–45.
5. Concessio N, Hickey A., Assessment of micronized powders dispersed as aerosols. Pharmaceutical Technology, 1994; 18(9): 88–98.
6. Rietema K., The dynamics of fine powders. London, UK: Elsevier Science Publishing Co., Inc. 1991; 123-132.
7. Concessio N, Oort M, Knowles M, Hickey A., Pharmaceutical dry powder aerosols: Correlation of powder properties with dose delivery and implications for pharmacodynamic effect, Pharmaceutical Research 1999; 16(6): 828–834.
8. Taylor M., Ginsburg J., Hickey A., Gheyas F., Composite method to quantify powder flow as a screening method in early tablet or capsule formulation development. AAPS Pharm Sci Tech 2000; 1(3): Article 18.
9. Pillai R., Yeates D., Miller I., Hickey A., Controlled dissolution from wax-coated aerosol particles in canine lungs, Journal of Applied Physiology 1998; 84(2): 717–725.
10. Sakagami M., In vivo, in vitro and ex vivo models to assess pulmonary absorption and disposition of inhaled therapeutics for systemic delivery, Advanced Drug Delivery Review 2006; 58: 1030–1060.
11. Pritchard J., The influence of lung deposition on clinical response, Journal of Aerosol Medicines 2001; 14: S19–S26.
12. Crowder T., Hickey A., Powder specific active dispersion for generation of pharmaceutical aerosols, International Journal of Pharmaceutics 2006; 327: 65–72.
13. Rehman M., Shekunov B., York P., Lechuga-Ballesteros D., Miller D., Tan T., Colthorpe P., Optimization of powders for pulmonary delivery using supercritical fluid technology, European Journal of Pharmaceutical Sciences 2004; 22: 1–17.
14. Chan H., Chew N., Novel alternative methods for the delivery of drugs for the treatment of asthma. Advanced Drug Delivery Review 2003; 55: 793–805.
15. Pauwels R., Newman S., Borgstrom L., Airway deposition and airway effects of antiasthma drugs delivered from metered-dose inhalers. European Respiratory Journal 1997; 10: 2127–2138.
16. Price D., Thomas M., Mitchell G., Niziol C., Featherstone R., Improvement of asthma control with a breath-actuated pressurized metred dose inhaler (BAI): a prescribing claims study of 5556 patients using a traditional pressurized metered dose inhaler (MDI) or a breathactuated device, Respiratory Medicines 2003; 97:12–19.
17. Cegla U., Pressure and inspiratory flow characteristics of dry powder inhalers, Respiratory Medicines 2004; 98: S22–S28.
18. Pillai R., Yeates D., Miller I., Hickey A., Controlled release from condensation coated respirable aerosol particles, Journal of Aerosol Sciences 1994; 25: 461–477.
19. Chan H., Chew N., Novel alternative methods for the delivery of drugs for the treatment of asthma, Advanced Drug Delivery Review 2003; 55: 793–805.
20. Elamin A., Ahlneck C., Alderborn G., Nystrom C., Increased metastable solubility of milled griseofulvin, depending on the formation of a disordered surface structure, International Journal of Pharmaceutics 1994;111: 159–170.
21. Ward G., Schultz R., Process-induced crystallinity changes in albuterol sulfate and its effect on powder physical stability, Pharmaceutical Research 1995; 12: 773–779.
22. Mackin L., Zanon R., Park J., Foster K., Opalenik H., Demonte M., Quantification of low levels (<10%) of amorphous content in micronised active batches using dynamic vapour sorption and isothermal microcalorimetry. International Journal of Pharmaceutics 2002; 231: 227–236.
23. Steckel H., Rasenack N., Villax P., Muller B.W., In vitro characterization of jet-milled and *in-situ*-micronized fluticasone-17-propionate, International Journal of Pharmaceutics 2003; 258: 65–75.
24. Bauer-Brandl A., Polymorphic transitions of cimetidine during manufacture of solid dosage forms, International Journal of Pharmaceutics 1996; 140: 195–206.

25. Brittain H.G., Effects of mechanical processing on phase composition, Journal of Pharmaceutical Sciences 2002; 91:1573–1580.
26. Heng J.Y.Y., Thielmann F., Williams D.R., The effects of milling on the surface properties of form I paracetamol crystals, Pharmaceutical Research 2006; 23: 1918–1927.
27. York P., Ticehurst M.D., Osborn J.C., Roberts R.J., Rowe R.C., Characterisation of the surface energetics of milled DL-propranolol hydrochloride using inverse gas chromatography and molecular modelling, International Journal of Pharmaceutics 1998; 174: 179–186.
28. Tong H.H.Y., Shekunov B.Y., York P., Chow A.H.L., Influence of polymorphism on the surface energetics of salmeterol xinafoate crystallized from supercritical fluids, Pharmaceutical Research 2002; 19: 640–648.
29. Cline D., Dalby R., Predicting the quality of powders for inhalation from surface energy and area, Pharmaceutical Research 2002; 19: 1274–1277.
30. Rogers T.L., Gillespie I.B., Hitt J.E., Fransen K.L., Crowl C.A., Tucker C.J., Kupperblatt G.B., Becker J.N., Wilson D.L., Todd C., Elder E.J., Development and characterization of a scalable controlled precipitation process to enhance the dissolution of poorly water soluble drugs, Pharmaceutical Research 2004; 21: 2048–2057.
31. Rasenack N., Steckel H., Muller B.W., Micronization of anti-inflammatory drugs for pulmonary delivery by a controlled crystallization process, Journal of Pharmaceutical Sciences 2003; 92: 35–44.
32. Rasenack N., Steckel H., Muller B.W., Preparation of microcrystals by in situ micronization, Powder Technology 2004; 143–144 , 291–296.
33. Ferrie A.R., Savage A.P., Novel apparatus and process for preparing crystalline particles, [WO0132125], United Kingdom, 2001.
34. Brenek S.J., Am Ende D.J., Crystallization method and apparatus using an an impinging plate assembly, Pfizer Products Inc., [WO 2004047797], United States of America, 2006.
35. Rasenack N., Muller B. W., Micro-size drug particles: common and novel micronization techniques, Pharmaceutical Development and Technology 2004; 9; 1 - 5.
36. Wang, Z., Chen, J. F., Le, Y., Shen, Z. G., Yun, J., Preparation of untrafine beclomethasone dipropionate drug powder by antisolvent precipitation. Ind. Eng. Chem. Res. 2007; 46: 4839 - 4843.
37. Millard J.W., Alvarez-Nunez F.A., Yalkowsky S.H., Solubilization by cosolvents: establishing useful constants for the log-linear model, International Journal of Pharmaceutics 2002; 245: 153–166.
38. Machatha S.G., Yalkowsky S.H., Bilinear model for the prediction of drug solubility in ethanol/water mixtures, Journal of Pharmaceutical Sciences 2005; 94: 2731–2734.
39. Sato T., Niwa H., Chiba A., Nozaki R., Dynamical structure of oligo(ethylene glycol)s water solutions studied by time domain reflectometry, Journal of Chemical Physics 1998; 108: 4138–4147.
40. Sailaja D., Raju K.N., Devi G.S.S., Subbarangaiah K., Ultrasonic behaviour of aqueous solutions of polyethylene glycols on the temperature of adiabatic compressibility minimum of water, European journal of Polymer 1998; 34: 887–890.
41. Noto V. Di, Longo D., Munchow V., Ion-oligomer interactions in poly(ethylene glycol)400/(LiCl)(x) electrolyte complexes, Journal of Physics and Chemical Biology 1999; 103: 2636–2646.
42. Begum R., Matsuura H., Conformational properties of short poly(oxyethylene) chains in water studied by IR spectroscopy, Journal of Chemical Society Faraday Trans.1997; 93: 3839–3848.
43. Telko, M. J.; Hickey, A. J. Dry powder inhaler formulation, Respiratory Care. 2005; 50: 1209 - 1210.
44. Ikegami, K.; Kawashima, Y.; Takeuchi, H.; Yamamoto, H.; Isshiki, N.; Mosose, D.; Ouchi, K. Primary crystal growth during spherical agglomeration in liquid: designing an ideal dry powder inhalation system, Powder Technology 2002; 126: 266 - 268.
45. Chew, N. Y. K.; Tang, P.; Chan, H. K.; Raper, J. A., How much partile surface corrugation is sufficient to improve aerosol performance of powders?, Pharmaceutical Research 2005; 22: 148-150.
46. Chan H.-K., Dry powder aerosol drug delivery-Opportunities for colloid and surface scientists, Colloids Surface A: Physicochemical Engineering Aspects 2006; 50: 284-285.
47. Raymond C R., Paul J S. and Siân C O., Pharmaceutical Excipients, 1545-1556.
48. Yu Z.Q., Chow P.S., Tan R.B.H., Application of attenuated total reflectance-Fourier transform infrared (ATR-FTIR) technique in the monitoring and control of anti-solvent crystallization, Industrial Engineering and Chemical Research 2006; 45: 438–444.
49. Franke J., Mersmann A., The influence of the operational conditions on the precipitation process, Chemical Engineering Sciences 1995; 50: 1737–1753.
50. Rodriguez-Hornedo N., Murphy D., Significance of controlling crystallization mechanisms and kinetics in pharmaceutical systems, Journal of Pharmaceutical Sciences1999; 88: 651–660.
51. Baldyga J., Bourne J.R., Hearn S.J., Interaction between chemical reactions and mixing on various scales, Chemical Engineering Sciences 1997; 52: 457–466.
52. Sedzik J., Regression analysis of factorially designed trials – a logical approach to protein crystallization, Biochim. Biophysics Acta 1995; 1251: 177–185.
53. Kawashima, Y.; Serigano, T.; Hino, T.; Yamamoto, H.; Takeuchi, H. Effect of surface morphology of carrier lactose on dry powder inhalation property of pranlukast hydrate. Int. J. Pharm., 1998; 172: 179 -182.

How to cite this article:
Uttekar PS and Chaudhari PD: Formulation and evaluation of engineered pharmaceutical fine particles of budesonide for dry powder inhalation (DPI) produced by amphiphilic crystallization technique: optimization of process parameters. *Int J Pharm Sci Res* 2013; 4(12): 4656-70. doi: 10.13040/IJPSR. 0975-8232.4(12).4656-70